

Experimental Study on Preparation of Magnesium Phosphate Cement from By-product Magnesium Slag of Spheroidizing Agent Industry

Siteng Hou, Shiyong Chen, Yiming Niu

Institute of Resources and Environment, Henan Polytechnic University, Jiaozuo 454000, China

Abstract

This paper mainly studied the preparation of magnesium phosphate cement (MPC) with spheroidizing agent industrial by-product magnesium slag (MSA) as the main raw material. The setting time, dry density, compressive strength, hydration products and microstructure were measured. The effects of different phosphorus/magnesium ratio $m(P)/m(M)$, water/binder ratio W/C , and dosage of retarder B/M on MPC performance and its mechanism were investigated. The test results show that with the decrease of $m(P)/m(M)$, the dry density increases gradually, and the compressive strength increases first and then decreases. With the increase of W/C , both dry density and compressive strength first increase and then decrease. When W/C is 50%, the compressive strength reaches the maximum. With the increase of B/M , the setting time is prolonged and the dry density increases gradually. When B/M is 1%, the compressive strength reaches the maximum, and the strength of 1d, 3d and 7d can reach 2.30MPa, 2.94MPa and 3.82MPa. The results of XRD and SEM analysis show that the hydration reaction is complete and more hydration products are produced. The addition of retarder delayed the hydration reaction time, made the MSA particles that did not participate in the reaction fill the pores, reduced the MPC cavity, and made the MPC more dense. More pores are formed to create a more stable pore structure, improving the MPC's performance.

Keywords

MSA; MPC; Hydration Product; Microstructure.

1. Introduction

MSA refers to industrial solid waste produced in the production of ferrosilicon rare-earth magnesium spheroidizing agent. In recent years, there has been a great demand for spheroidizing agents, and at the same time, the number of Msas has been increasing. As the main component of MSA is MgO, accumulated MSA may cause some serious environmental problems. Fine magnesium slag particles may be blown away by the wind, resulting in dust pollution and harm to human respiratory system. The polluting extracts of MSA may contaminate groundwater by penetrating porous subsoil. At the same time, a large amount of accumulated MSA also causes resource waste and ecological environment destruction. However, there are few researches on MSA at present. From the perspective of environment and economy, the comprehensive utilization of MSA is an important way to improve the efficiency of resource utilization and promote sustainable development.

Magnesium phosphate cement (MPC) is a chemically bound ceramic formed by acid-base reaction between magnesium oxide (MgO) and soluble acid phosphate ($NH_4H_2PO_4$ or KH_2PO_4)[1]. Take KH_2PO_4 (KDP) as an example, its main reaction equation is as follows:

Compared with traditional Portland cement, MPC has many unique advantages, such as rapid setting and hardening[2], high early strength[3], good adhesion[4], low drying shrinkage[5], excellent wear resistance and freeze-thaw resistance[6], resistance to sulfate attack[7], and used for curing heavy metals[8]. In addition, it produces less carbon dioxide emissions during production and is considered a suitable alternative to OPC. So far, MPCs have been widely used in the rapid repair of building structures, concrete roads, Bridges, runways and floors[9-10]. Biomedical[11] and Structure strengthening[12], 3D Printing materials[13], Protective coating materials[14], Supercapacitor materials[15], harmful element solidification/stabilization (S/S) cementification materials[16].

As the main raw material of MPC, MgO plays an important role in its performance. The main way to produce MgO is to calcination of magnesite (MgCO₃). In MPC production, dead burning of magnesite at a calcination temperature above 1000°C is preferred, because higher calcination temperature can make the surface oxide layer of MgO denser, thus slowing down the hydration reaction rate and improving the performance of MPC[17]. However, the reserves of magnesite are very rare and only found in a few countries and regions. On the distribution of magnesite, magnesite is characterized by uneven distribution, more than 84% of magnesite reserves of our country is concentrated in Liaoning Province[18]. With the rapid development of China's economy, the demand for magnesite has increased sharply in recent years. The mining of magnesite includes grinding, ore concentration, waste dumping and other processes[19]. If the mining process is not managed, the soil quality in the mining area may be adversely affected. Due to its high calcination temperature, the limitation of raw material distribution, and the possible environmental pollution in the mining process, the production cost will increase. Therefore, finding new low-cost materials as the source of magnesium in MPC is an important issue to reduce its production cost and expand its application range.

In this study, MSA was taken as the main raw material for MPC production, and its impact on MPC characteristics was studied. The setting time, dry density and mechanical properties of MPCs under different phosphorus/magnesium ratios ((m)P/(m)M), water-binder ratio (W/C) and retarder dosage (B/M) were characterized. The hydration products and microstructure of MPC were analyzed by X-ray diffraction (XRD) and scanning electron microscopy (SEM).

2. Materials and Test Methods

2.1 The Main Raw Material for the Test

In this study, MgO is selected instead of MSA, and its main components are shown in Table 1, and its particle size distribution is shown in Figure 1. KDP is industrial grade potassium dihydrogen phosphate, white crystal, purity >90%, retarder is industrial grade borax (Na₂B₄O₇·10H₂O), analytical pure, white crystal, purity ≥99.5%, produced by Tianjin Damao Chemical Reagent Factory, mixing water is tap water, temperature at (20±1) °C.

Table 1. Main chemical components of MSA

composition	MgO	SiO ₂	Al ₂ O ₃	CaO	Fe ₂ O ₃	other
content%	81.64	11.77	2.93	0.377	1.52	1.763

Figure 1 shows the particle size distribution of MSA, in which the median particle size (D₅₀) is 2.58µm, and the particle size (D₉₀) of most particles is below 42.6µm. Its main particle size is about 1µm, and its specific surface area is 2035 m²/kg. Compared with the MgO obtained from calcined magnesite, the MSA has smaller particle size and larger specific surface area. This can better fill the MPC hole during the reaction, making the sample more dense.

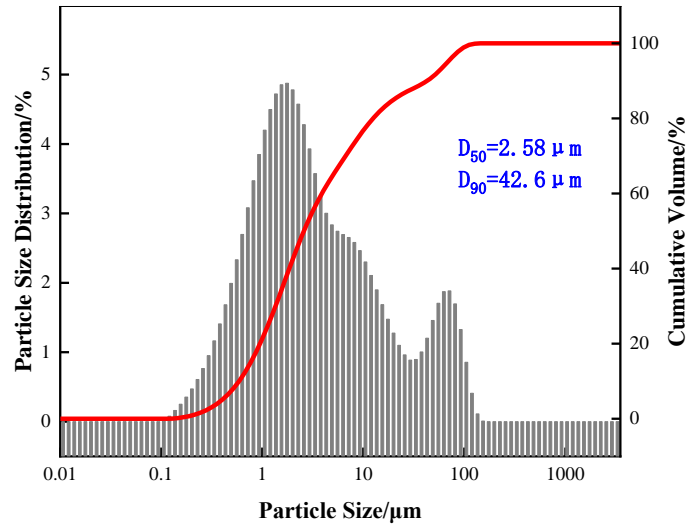


Figure 1. Particle size distribution of MSA

2.2 Preparation of Sample

Firstly, each component of magnesium phosphate cement is accurately weighed according to the mix ratio, and each component is mixed and poured into the mixing pot. The cement cement sand mixer is used to slowly stir for 30 s, and each component is evenly mixed. After that, weigh tap water according to the water-glue ratio and pour it into the mixing pot. Stir until all components are evenly mixed. Pour the clean pulp into a triple test mold of 40 mm×40 mm×160 mm according to GB/T 17671-2021 "Test Method for Cement Mortar Strength". The excess bubbles in the clean slurry were discharged on the shaking table to make the slurry mixed evenly. After 1h, the slurry was removed and placed in a natural environment for curing.

3. Results and Discussion

3.1 Impact of m(P)/m(M) on MPC Performance

Table 2. Ratio of raw materials

number	1	2	3	4	5	6	7	8	9	10
m(P)/m(M)	1:1	1:2	1:3	1:4	1:5	1:6	1:7	1:8	1:9	1:10
B/M(%)	0	0	0	0	0	0	0	0	0	0
W/C(%)	50	50	50	50	50	50	50	50	50	50

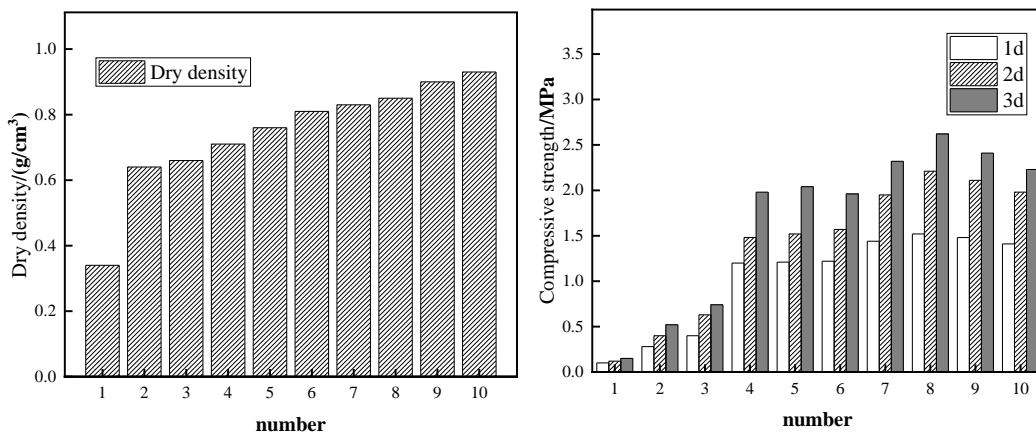


Figure 2. Effects of m(P)/m(M) on dry density (left) and compressive strength (right)

Figure 2 shows the influence of $m(P)/m(M)$ on dry density (left) and compressive strength (right). It can be seen from the image that with the decrease of $m(P)/m(M)$, the dry density of the prepared sample keeps increasing, and the compressive strength increases first and then decreases. Between 1/4 and 1/6, the late strength increased significantly; between 1/7 and 1/8, the early strength of the specimen increased gradually, but the late strength increased slightly, indicating that when $m(P)/m(M)$ was 1/4 to 1/6, more hydration products were continuously produced in the curing process. Between 1/7 and 1/8, MgO content increased with the decrease of $m(P)/m(M)$. MgO, which did not participate in the reaction, filled the pores, resulting in a denser sample and improved the overall strength of the sample. The content of KDP was reduced, and the hydration products produced by the continuous reaction were less, resulting in a low strength improvement in the process of continuous hydration. From 1/9 to 1/10, the strength of the sample in the early stage began to decrease, and the strength increase in the late stage continued to decrease, indicating that as the content of KDP continued to decrease, the hydration products generated by the continuous reaction became less and less, and it was difficult to wrap the remaining MgO, resulting in the overall strength of the sample decreased.

Figure 3 shows XRD images of different $m(P)/m(M)$. It can be seen from Figure 3 that the main crystal components of MPC are MgO and $MgKPO_4 \cdot 6H_2O$. With the decrease of $m(P)/m(M)$, the diffraction peak intensity of $MgKPO_4 \cdot 6H_2O$ decreases continuously, while the diffraction peak intensity of MgO increases continuously. This indicates that with the decrease of $m(P)/m(M)$, less hydration products are produced, which is consistent with the analysis results in Figure 2. When $m(P)/m(M)$ is 1/1, a large amount of hydration products are produced. However, due to the excessive reaction, a large amount of heat is generated during the reaction process, which leads to the excessive water loss of MPC and the formation of a large number of unstable pores, leading to the collapse of the overall structure. When $m(P)/m(M)$ is 1/5, the content of hydration products of MPC is higher, and a stable pore structure is generated during hydration heat release.

Figure 4 shows the SEM images with $m(P)/m(M)$ as 1/5(left) and 1/8(right), from which it can be observed that when $m(P)/m(M)$ is 1/5, more hydration products and relatively stable pore structure are produced, while when $m(P)/m(M)$ is 1/8, it can be observed that fewer hydration products are produced, and MgO, which does not participate in the reaction, fills the pores. This is consistent with the above analysis results.

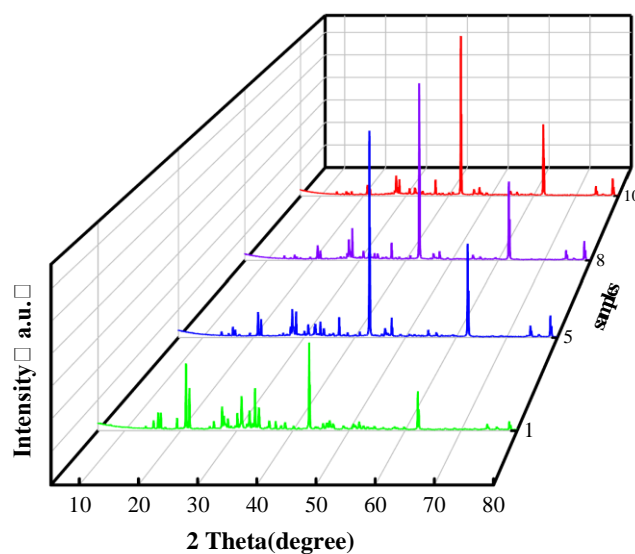


Figure 3. XRD images of different $m(P)/m(M)$

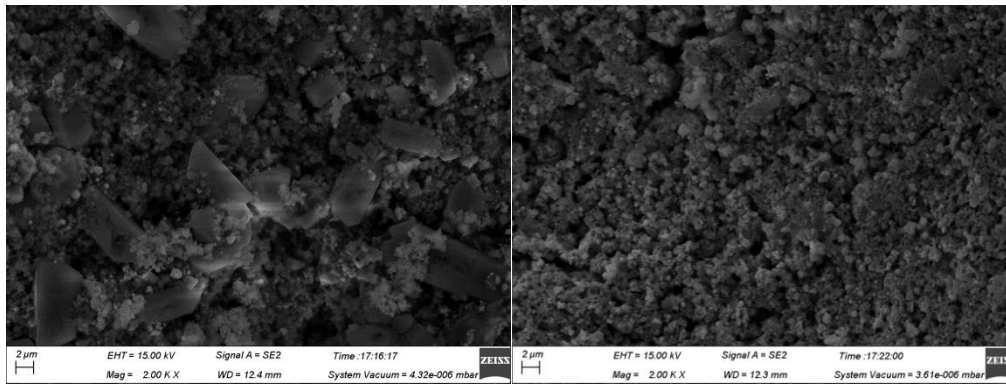


Figure 4. SEM images with m(P)/m(M) values of 1:5(left) and 1:8(right)

3.2 Effect of W/C on MPC Performance

Table 3. Ratio of raw materials

number	W-30	W-40	W-50	W-60	W-70
m(P)/m(M)	1:5	1:5	1:5	1:5	1:5
B/M(%)	0	0	0	0	0
W/C(%)	30	40	50	60	70

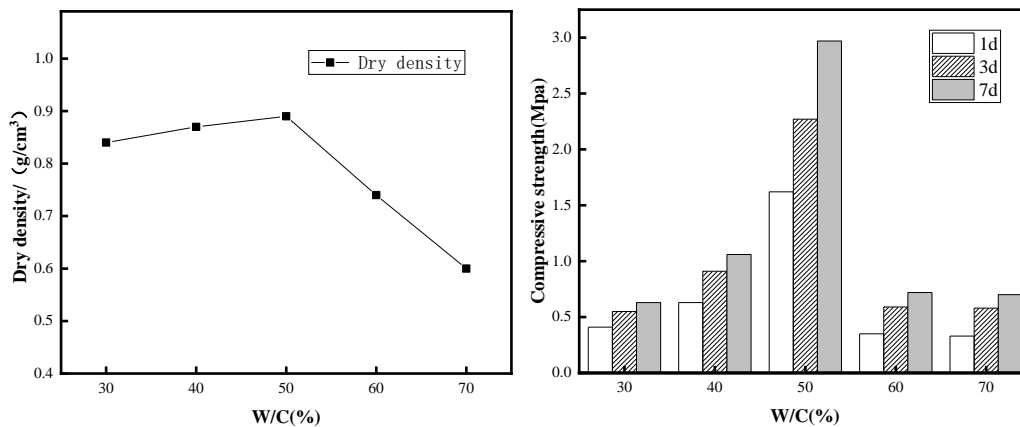


Figure 5. Images of dry density (left) and compressive strength at different W/C (right)

As can be seen from Figure 5, with the increase of W/C, the compressive strength and dry density of each age increase first and then decrease. When W/C is below 50%, the change of compressive strength is large, but the change of dry density is small. When W/C is above 50%, the change of compressive strength and dry density is large. This is due to the rapid hydration reaction of MPC and the release of a large amount of heat. When W/C is below 50%, the cement slurry is thicker, difficult to mix evenly in the mixing process, at the same time, the water loss is too fast, resulting in inadequate reaction, less hydration products, resulting in a slight reduction in dry density, but the compressive strength is greatly reduced. When W/C increases to 50%, the fluidity of cement slurry is better, and the mixture can be fully moistened to produce more uniform pores. When W/C continues to increase, because the excess water does not participate in the hydration reaction, the excess water evaporates during the curing process, forming pores in the interior, resulting in a substantial reduction in dry density and compressive strength.

Figure 6 shows XRD images of different W/C. It can be seen from Figure 6 that when W/C is 40%, the diffraction peak intensity of $MgKPO_4 \cdot 6H_2O$ is low, indicating that less hydration products are produced at this time. When W/C is 60%, the diffraction peak intensity of MgO is low, which is

because there is more free water that does not participate in the reaction in the mixing process, leading to the reduction of MgO content, which is consistent with the analysis results in Figure 5.

Figure 7 shows the SEM images with W/C of 50% (left) and 60% (right). It can be observed from the images that a relatively stable pore structure is generated when W/C is 50%, while there are more irregular large pores when W/C is 60%, which affects the overall compressive strength, which is consistent with the above analysis results.

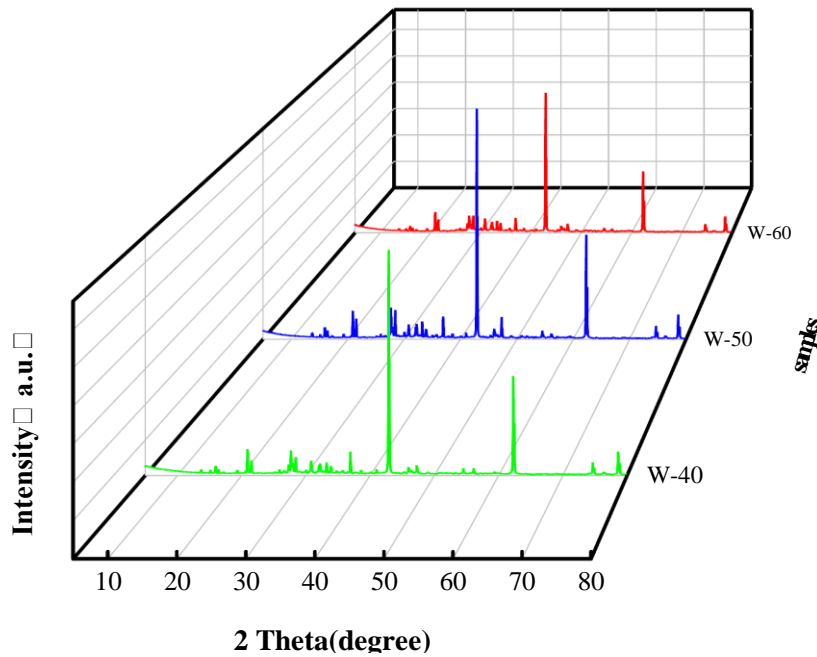


Figure 6. XRD images with water-binder ratio of 40%, 50% and 60%

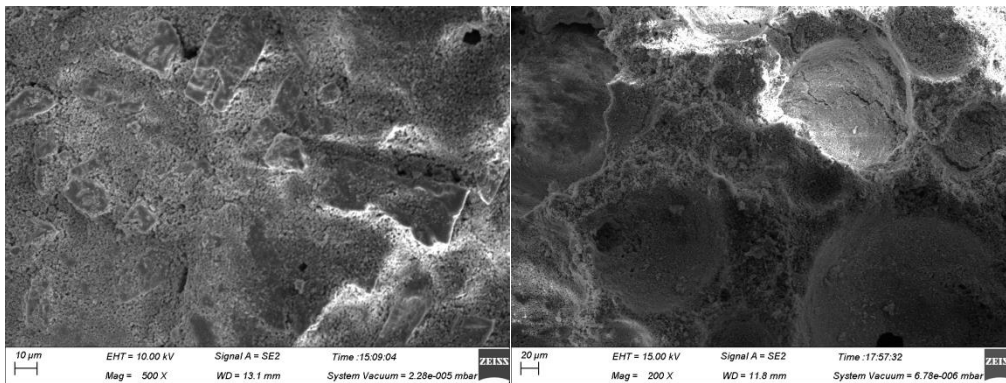


Figure 7. SEM images with W/C of 50%(left) and 60%(right)

3.3 3.3 Effect of B/M on MPC

Table 4. Ratio of raw materials

number	W-50	B-0.5	B-1	B-1.5	B-2	B-2.5
m(P)/m(M)	1:5	1:5	1:5	1:5	1:5	1:5
B/M(%)	0	0.5	1	1.5	2	2.5
W/C(%)	50	50	50	50	50	50
Setting time(min)	1	1.5	2	2.5	3.5	4.5

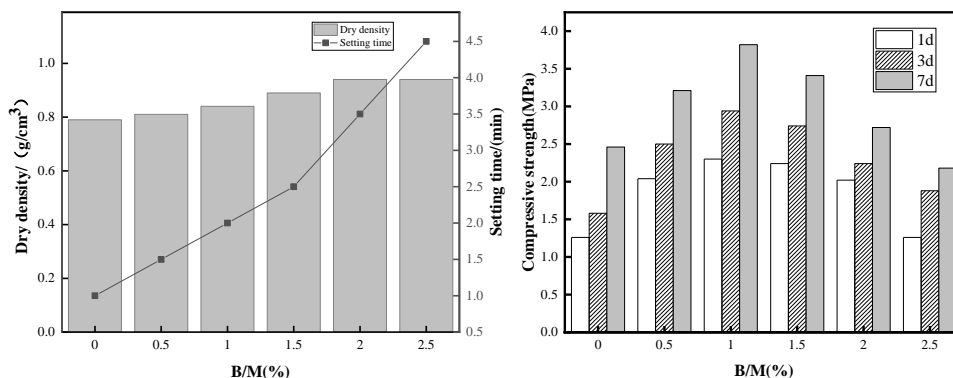


Figure 8. Images of dry density-setting time (left) and compressive strength (right) at different B/M

The setting and hardening time of MPC is too fast and the operation time is short. If no retarder is added, it cannot meet the requirements of site construction. As can be seen from Figure 8, with the increase of B/M, the setting time keeps increasing, and the dry density first increases and then becomes stable. The compressive strength of all ages increases first and then decreases, and the compressive strength of all ages reaches the maximum when B/M is 1%. This is due to the strong alkaline water solution of borax, easy and KDP dissolved in water and water dissociated H⁺ acid-base neutralization reaction. In addition, with the advance of the reaction, the acid ions and H⁺ in the solution are constantly reduced, which hinders the dissolution of MgO particles[20]. At the same time, B₄O₇²⁻ ions in the mixed solution can be rapidly absorbed by MgO particles and combine with Mg²⁺ ions in MPCMP slurry to form precipitation and become a protective film of hydration products. The membrane may prevent Mg²⁺ ions formed by dissolved MgO particles from contacting K⁺ ions and H₂PO₄⁻ ions in MPC slurry, resulting in low early hydration rate of MPC. Therefore, with the increase of B/M, the setting time keeps lengthening[21]. The addition of borax leads to the decrease of hydration exothermic heat and the extension of hydration reaction. Due to the decrease of pores produced in the production process of hydration products, the dry density keeps increasing. When there are almost no pores inside the material, the change of dry density tends to be stable. When B/M is less than 1%, the addition of borax improves the pore structure and the compressive strength of MPC. With the increase of B/M, the amount of MgO involved in the reaction decreases, which leads to the decrease of the compressive strength.

Figure 9 shows XRD images with different W/C. It can be seen from Figure 9 that when B/M is 0, the diffraction peak intensity of MgKPO₄·6H₂O and MgO are both higher, indicating that more hydration products are generated and more MgO is not involved in the reaction. This is because when no retarder is added, the hydration reaction speed is fast, resulting in fast water loss in the reaction process, resulting in more MgO not involved in the reaction. When B/M is 0.5%, 1% and 2.5%, the diffraction peak intensity of MgKPO₄·6H₂O has little difference, while the diffraction peak intensity of MgO gradually increases. For the same reason mentioned above, with the addition of borax, the amount of MgO involved in the reaction decreases continuously, resulting in the increasing intensity of the diffraction peak of MgO.

Figure 10 shows the SEM images with B/M of 0% and 1%. It can be observed from the images that when B/M is 0%, a large number of hydration products are produced, while a large number of irregular pores and MgO that do not participate in the reaction are observed. This is because a large number of unstable pores are formed when borax is not added and hydration reaction time is fast. In addition, because the setting time of MPCMP slurry is fast and the stirring is uneven, the MgO which does not participate in the reaction has no time to fill the pores, thus affecting the overall strength. When B/M is 1%, it can be observed that a relatively stable pore structure is formed. This is because the addition of borax extends the reaction time, makes the slurry mix more evenly, delays the hydration reaction, forms a more stable pore structure and improves the overall strength, which is consistent with the conclusion above.

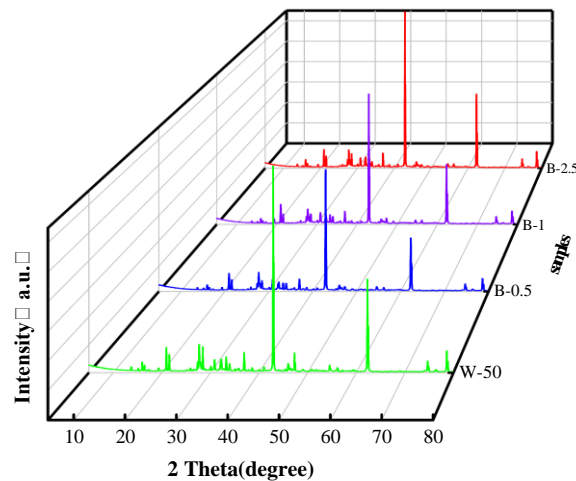


Figure 9. XRD images at B/M values of 0%, 0.5%, 1% and 2.5%

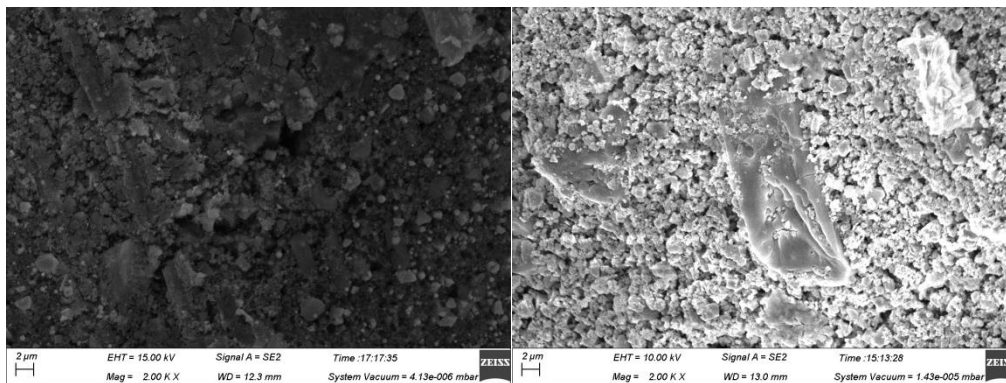


Figure 10. XRD images when B/M is 0% and 1%

4. Conclusion

(1) With $m(P)/m(M)$ decreasing, the dry density of MPC increases, and the compressive strength increases first and then decreases, reaching the maximum when $m(P)/m(M)$ is $1/8$. However, according to the results of XRD and SEM analysis, fewer hydration products are produced at this time, and the reason for the high strength is that MgO involved in the reaction blocked the pores inside the material, making the material denser and thus improving the compressive strength. When $m(P)/m(M)$ is greater than $1/5$, the hydration reaction is too fast, and a large number of unstable pores are formed in the reaction process, resulting in the collapse of the overall structure of the material. However, when $m(P)/m(M)$ is $1/5$, the hydration reaction is more complete and more hydration products are produced.

(2) With the increasing of W/C, the dry density of MPC first increases and then decreases, and the compressive strength first increases and then decreases. As can be seen from XRD analysis results, hydration reaction is insufficient when water is less, resulting in low dry density and low compressive strength of materials. According to the SEM analysis results, when there is more water, the water that does not participate in the reaction will evaporate a large number of pores, leading to the decrease of dry density and compressive strength. When B/M is 50%, more hydration products are generated and a relatively stable pore structure is formed. At this time, the dry density and compressive strength reach the maximum.

(3) With the increase of B/M, the dry density of MPC increases and the compressive strength increases first and then decreases. According to the XRD analysis results, the hydration reaction time was delayed at the beginning due to the addition of retarder, the slurry was mixed more evenly in the

stirring process, the MgO that did not participate in the reaction was reduced, and a more stable pore structure was formed in the reaction process, leading to the increasing dry density. With the addition of retarder, the MgO which did not participate in the reaction increased, resulting in the decrease of the compressive strength of the material. At the same time, the hydration reaction time is longer, the material has almost no porosity, and the change of dry density tends to be stable. When B/M is 1%, the compressive strength reaches the maximum, and a more uniform and stable pore structure can be observed under SEM.

References

- [1] Walling Sam A, Provis John L. Magnesia-Based Cements: A Journey of 150 Years, and Cements for the Future?[J]. *Chemical reviews*, 2016, 116(7).
- [2] M. Aminul Haque, Bing Chen. Research progresses on magnesium phosphate cement: A review[J]. *Construction and Building Materials*, 2019, 211.
- [3] Amit Arora, Birpal Singh, Parampreet Kaur. Novel material i.e. magnesium phosphate cement (MPC) as repairing material in roads and buildings[J]. *Materials Today: Proceedings*, 2019, 17(Pt 1).
- [4] Jihui Qin, Jueshi Qian, Chao You, Yingru Fan, Zhen Li, Hongtao Wang. Bond behavior and interfacial micro-characteristics of magnesium phosphate cement onto old concrete substrate[J]. *Construction and Building Materials*, 2018, 167.
- [5] Fei Qiao, C.K. Chau, Zongjin Li. Property evaluation of magnesium phosphate cement mortar as patch repair material[J]. *Construction and Building Materials*, 2009, 24(5).
- [6] Linchun Zhang, Ailian Zhang, Qian Wang, Yan Han, Ke Li, Xiaojian Gao, Zhenyu Tang. Corrosion resistance of wollastonite modified magnesium phosphate cement paste exposed to freeze-thaw cycles and acid-base corrosion[J]. *Case Studies in Construction Materials*, 2020, 13.
- [7] Li Jun, Ji Yongsheng, Zhang Linglei, Liu Benlin. Resistance to sulfate attack of magnesium phosphate cement-coated concrete[J]. *Construction and Building Materials*, 2019, 195.
- [8] Irene Buj, Josep Torras, Miquel Rovira, Joan de Pablo. Leaching behaviour of magnesium phosphate cements containing high quantities of heavy metals[J]. *Journal of Hazardous Materials*, 2009, 175(1).
- [9] Ban Jin, Longzhu Chen, Bing Chen. Factors assessment of a repair material for brick masonry loaded cracks using magnesium phosphate cement[J]. *Construction and Building Materials*, 2020, 252(C).
- [10] Liu Fei, Pan Baofeng, Zhou Changjun. Experimental Study on a Novel Modified Magnesium Phosphate Cement Mortar Used for Rapid Repair of Portland Cement Concrete Pavement in Seasonally Frozen Areas[J]. *Journal of Materials in Civil Engineering*, 2022, 34(3).
- [11] Maryam Nabiyouni, Theresa Brückner, Huan Zhou, Uwe Gbureck, Sarit B. Bhaduri. Magnesium-based bioceramics in orthopedic applications[J]. *Acta Biomaterialia*, 2018, 66.
- [12] Zhu Cheng Jie, Fang Shuai, Ng P. L., Pundiené Ina, Chen Jia Jian. Flexural Behavior of Reinforced Concrete Beams Strengthened by Textile Reinforced Magnesium Potassium Phosphate Cement Mortar[J]. *Frontiers in Materials*, 2020, 7.
- [13] Yiwei Weng, Shaoqin Ruan, Mingyang Li, Liwu Mo, Cise Unluer, Ming Jen Tan, Shunzhi Qian. Feasibility study on sustainable magnesium potassium phosphate cement paste for 3D printing[J]. *Construction and Building Materials*, 2019, 221.
- [14] Jun Li. Improvement in Water Resistance of MAPC Coatings as Function of NaCl Concentration[J]. *Emerging Materials Research*, 2019, 8(3).
- [15] Weiyuan Ma, Dong Zhang. Multifunctional structural supercapacitor based on graphene and magnesium phosphate cement[J]. *Journal of Composite Materials*, 2019, 53(6).
- [16] Xing Cao, Rui Ma, Qiushi Zhang, Weibing Wang, Qinxiong Liao, Shichang Sun, Peixin Zhang, Xiangli Liu. The factors influencing sludge incineration residue (SIR)-based magnesium potassium phosphate cement and the solidification/stabilization characteristics and mechanisms of heavy metals[J]. *Chemosphere*, 2020, 261.
- [17] Jincheng Yu, Jueshi Qian, Fan Wang, Zhen Li, Xingwen Jia. Preparation and properties of a magnesium phosphate cement with dolomite[J]. *Cement and Concrete Research*, 2020, 138.

- [18] Jincheng Yu, Jueshi Qian, Fan Wang, Jihui Qin, Xiaobing Dai, Chao You, Xingwen Jia. Study of using dolomite ores as raw materials to produce magnesium phosphate cement[J]. Construction and Building Materials, 2020, 253(C).
- [19] Jincheng Yu, Jueshi Qian, Fan Wang, Jihui Qin, Xiaobing Dai, Chao You, Xingwen Jia. Study of using dolomite ores as raw materials to produce magnesium phosphate cement[J]. Construction and Building Materials, 2020, 253(C).
- [20] Nan Yang, Caijun Shi, Jianming Yang, Yuan Chang. Research Progresses in Magnesium Phosphate Cement-Based Materials[J]. Journal of Materials in Civil Engineering, 2013, 26(10).
- [21] Jin Bao Wen, Li Xia Zhang, Xiu Sheng Tang, Guo Hong Huang, Ye Ran Zhu. Effect of Borax on Properties of Potassium Magnesium Phosphate Cement[J]. Materials Science Forum, 2018, 4596.